DOE/JPL/954901-2

DEVELOPMENT AND EVALUATION OF DIE MATERIALS FOR USE IN THE GROWTH OF SILICON RIBBONS BY THE INVERTED RIBBON GROWTH PROCESS—TASK II—LSSA PROJECT

Quarterly Report No. 2

By
M. T. Duffy
S. Berkman
G. W. Cullen

March 1978

Work Performed Under Contract No. NAS-7-100-954901

RCA Laboratories
Princeton, New Jersey

U.S. Department of Energy

Solar Energy

DISCLAIMER

NOTICE

DOE/JPL/954901-2
Distribution Category UC-63e

DEVELOPMENT AND EVALUATION OF DIE MATERIALS FOR USE IN THE GROWTH OF SILICON RIBBONS BY THE INVERTED RIBBON GROWTH PROCESS — TASK II — LSSA PROJECT

M. T. Duffy, S. Berkman,
and G. W. Cullen
RCA Laboratories
Princeton, New Jersey 08540

QUARTERLY REPORT NO. 2

March 1978

This work was performed for the Jet Propulsion Laboratory, California Institute of Technology, under NASA Contract NAS7-100 for the Department of Energy.

The JPL Low-Cost Silicon Solar Array Project is funded by DOE and forms part of the DOE Photovoltaic Conversion Program to initiate a major effort toward the development of low-cost solar arrays.

Prepared Under Contract No. 954901 For
JET PROPULSION LABORATORY
CALIFORNIA INSTITUTE OF TECHNOLOGY
Pasadena, California 91103

PREFACE

This Quarterly Report No. 2, prepared by RCA Laboratories, Princeton, NJ 08540, describes work performed for the period 1 January 1978 through 31 March 1978, under Contract No. 954901 in the Materials and Processing Research Laboratory, H. Kressel, Director. G. W. Cullen is the Group Head and the Project Supervisor. M. T. Duffy is the Project Scientist. Others who participated in the research and/or writing of this report are S. Berkman, R. V. D'Aiello, K. M. Kim, P. J. Zanzucchi, J. F. Corboy, R. J. Paff, M. Popov, R. A. Soltis, and H. E. Temple. The RCA Report No. is PRRL-78-CR-13.

The JPL Project Monitor is T. O'Donnell.

TABLE OF CONTENTS

LIST OF ILLUSTRATIONS

SECTION I

SUMMARY

Silicon sessile drop experiments were performed on mullite and beryllia substrates both with and without a chemically vapor deposited-silicon nitride (CVD-Si_3N_4) coating. The mullite substrate caused doping of the silicon droplet to a resistivity of about 0.06 Ω-cm after heating for 1 h at 1450°C. The presence of a nitride later, though cracked, resulted in a resistivity of about 0.25 Ω-cm under similar conditions. In the case of beryllia the samples shattered upon cooling and measurements were not possible. Molten silicon in contact with both substrates displayed high contact angles.

Results of x-ray analysis on the thermal stability of Si_3N_4, both in the presence and absence of molten silicon, show that the as-prepared amorphous layers are converted predominantly to the α phase with high temperature treatment. The α phase is then slowly converted to the β phase accompanied by simultaneous decomposition. The latter process appears to occur more rapidly in contact with the silicon melt than in an inert gas. In both cases the β phase seems to be the more stable form of Si_3N_4.

Silicon ribbon specimens doped with boron (ρ = 1 Ω-cm) were grown from dies coated with Si_3N_4 for solar cell fabrication. Infrared analysis of two such ribbon specimens indicated that the oxygen and carbon content were below the level of detection. The Czochralski seed material was used as a reference, and the analysis showed an oxygen level of ∿35 ppma and 30-40 ppma for carbon in the latter. By comparison, the levels in the grown ribbon were estimated to be < 5 ppma for oxygen and < 25 ppma for carbon.

Solar cells without AR coatings, fabricated in two ribbon samples, gave efficiencies of 6.6% and 8.0%, respectively, relative to 9.6% for a Czochralski control. The application of an AR coating increased the efficiency of the best ribbon cell from 8.0 to 11.8%.

SECTION II

INTRODUCTION

The objective of this program is to develop and evaluate die materials for use in the growth of silicon ribbons by the inverted ribbon growth process (IRG). The major emphasis is on developing CVD coatings of Si_3N_4 and SiO_xN_y on suitable die materials and studying the stability and interaction of these layers with molten silicon. The dies are being tested in silicon ribbon growth experiments. The ribbons are being characterized electrically, crystallographically, and in solar cells. Self-supporting CVD dies and crucibles will also be fabricated, and deposition parameters will be adjusted, where possible, to favor minimum cost. Other potentially useful materials will be prepared and tested.

SECTION III

PROGRESS AND TECHNICAL DISCUSSION

A. SESSILE DROP EXPERIMENTS ON SUBSTRATE MATERIALS AND CVD-COATED SUBSTRATES

In previous experiments we have examined the potential of various commercially available refractory materials, including carbides, nitrides and oxides, for contact with molten silicon. Two interesting materials were not included in the above evaluation, namely, beryllia and mullite. During this reporting period, silicon sessile drop experiments were performed on beryllia and glass-rich mullite (85% mullite + 15% glass) substrates both with and without CVD-Si_3N_4 coatings (NH_3:SiH_4 = 33:1). Sectioned silicon/mullite samples gave a four-point-probe reading for silicon resistivity of approximately 0.05 Ω-cm after heating at 1450°C in ultrapure helium for 1 h. The corresponding resistivity for Si/Si_3N_4/mullite sectioned samples was approximately 0.3 Ω-cm irrespective of whether the substrate was coated on one or both sides. Microscopic examination revealed, however, that the nitride layer under the silicon was cracked, allowing the molten silicon to contact the substrate in the cracks as shown in Fig. 1. In the case of beryllia the silicon droplet shattered from the substrate in the cooling-down process, and resistivity measurement was not possible. Both the Si_3N_4 layer and silicon droplet shattered during the cooling of CVD-coated beryllia substrates. Molten silicon in contact with both substrate materials displayed high contact angles.

B. STABILITY OF CVD MATERIALS

Work commenced this reporting period on a more detailed analysis of the composition and stability of CVD-Si_3N_4 layers. A layer of nitride was removed from the susceptor on which the die parts, used in the growth of silicon ribbon, were coated. This layer represented several deposition runs with the ratio NH_3:SiH_4 = 33:1. The susceptor had been coated originally with a layer of silicon which was selectively etched from the back of the nitride to provide a free-standing silicon nitride layer. A portion of this layer was heated at 1500°C in ultrapure He for 30 min and was then examined

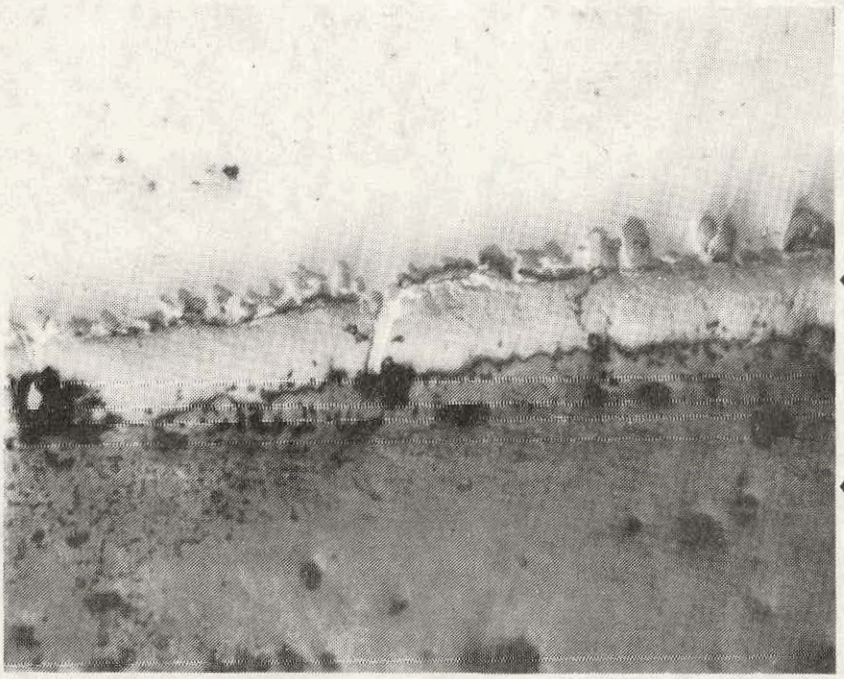

~ 275X

Figure 1. Section micrograph of a Si/CVD-Si_3N_4/mullite sample showing cracked CVD layer

by x-ray diffraction (powder pattern) for identification of the phases present and estimated content. This procedure was then repeated for successively longer periods of time up to a total of 30 h. The results are tabulated below.

TABLE 1. PHASES PRESENT IN CVD-Si_3N_4 LAYER AFTER HEATING AT 1500°C FOR SUCCESSIVELY LONGER PERIODS OF TIME

Approximate Content			Time at 1500°C
α-Si_3N_4	β-Si_3N_4	Si	hours
80%	20%	--	0.5
75%	20%	5%	3
75%	20%	5%	5.5
15%	40%	45%	30

There is an apparent transition from the α phase to the β phase accompanied by decomposition. It is interesting to note that there is a relative increase in the β-phase content despite the fact that decomposition is also taking place. Microscopic examination of the polished section of the same layer, after heating for 34 h at 1500°C in He, showed that the sample had a porous texture on both surfaces while apparently quite dense in the center region of the sample. This is shown in Fig. 2, where micrograph (a), taken with angular illumination, shows the two porous edges and central region of the cross section of the layer. Micrograph (b), taken with perpendicular illumination, shows the higher reflectance of the central coherent region relative to the porous edges of the cross section. X-ray powder patterns were obtained on specimens from the three regions - both faces of the sample and central region. The results are tabulated below. A portion of the same sample was etched in a mixture of HNO_3 + HF to remove excess silicon which might be accessible to the etchant, and x-ray powder patterns again obtained on the corresponding three regions. The results are also tabulated in Table 2. The designation front surface in Table 2 refers to the surface which was exposed to the gaseous reagents during the CVD process, and was exposed to the He ambient during heat treatment. The back surface corresponds to that which was in contact with the susceptor during deposition and rested on a vitreous carbon support during heat treatment in He.

TABLE 2. PHASES PRESENT IN CVD-Si_3N_4 LAYER AFTER HEATING AT 1500°C FOR 34 HOURS IN HELIUM

	Approximate Content (before etching)			Approximate Content (after etching)		
	α-Si_3N_4	β-Si_3N_4	Si	α-Si_3N_4	β-Si_3N_4	Si
Front Surface	45%	15%	40%*	70%	30%	∿1%
Central Region	25%	45%	30%	33%	66%	∿1%
Back Surface	14%	43%	43%	25%	75%	∿1%

*Most of the silicon present here could be observed microscopically as clustered particles on the sample surface and was not uniformly distributed throughout the surface region.

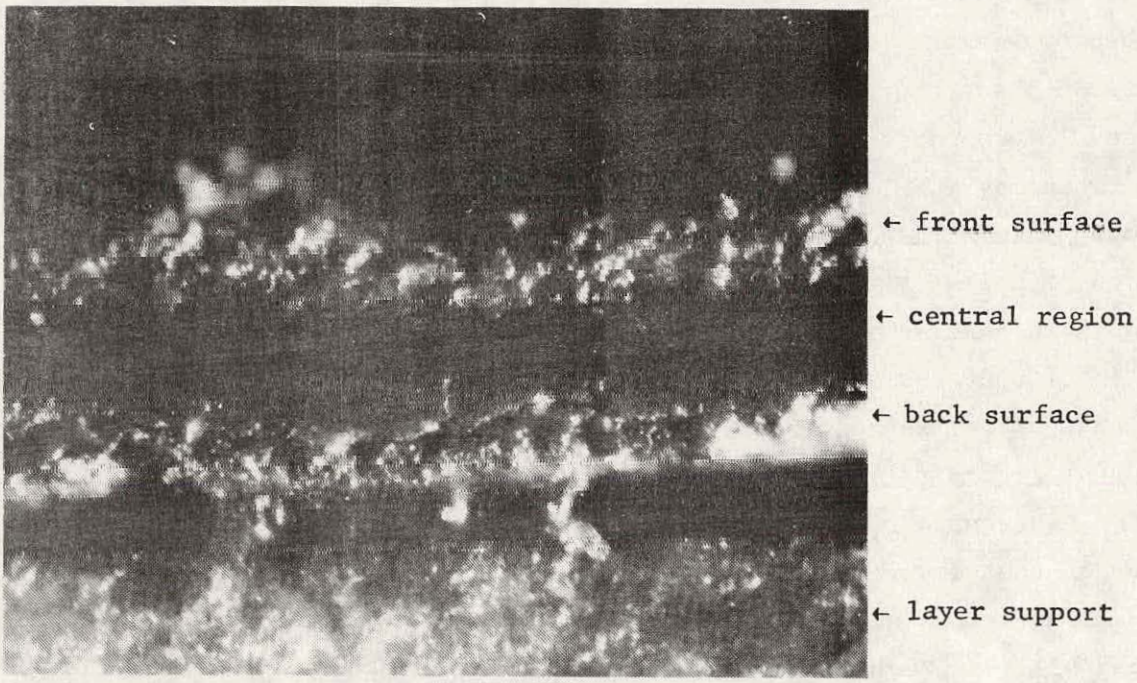

(a) ~135X

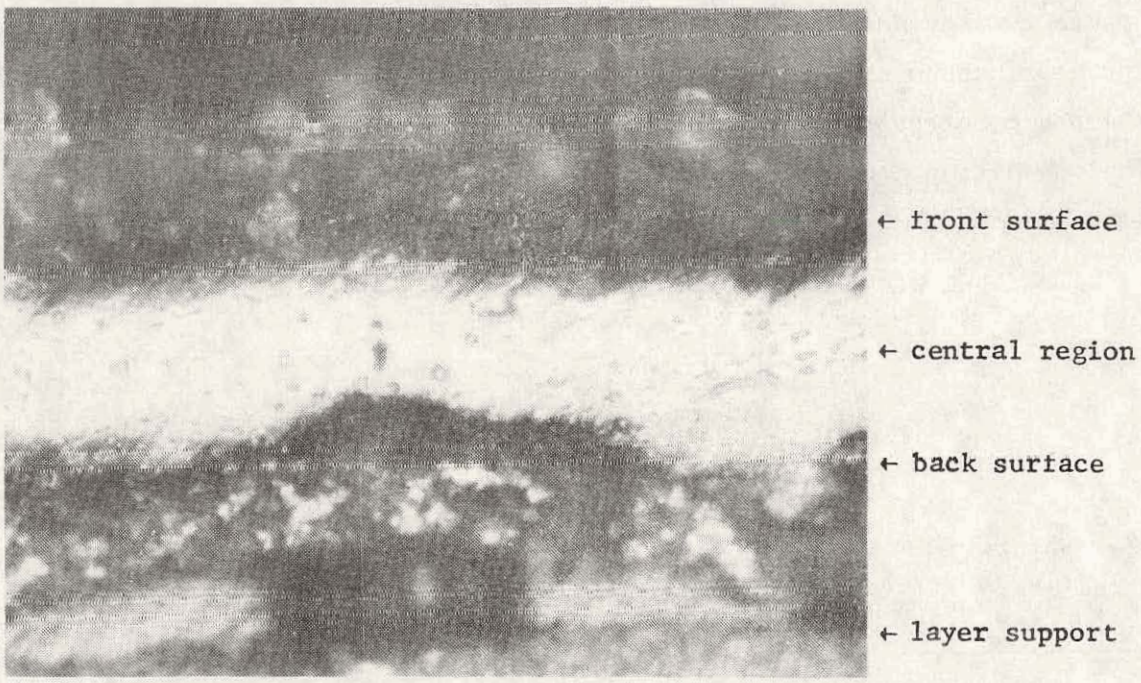

(b) ~135X

Figure 2. Section micrograph of a CVD-Si_3N_4 layer after heating in He at 1500°C for 34 h; (a) micrograph taken with perpendicular illumination, (b) with angular illumination.

The results presented in Table 2 show variation in content between the different regions of the film. This obscures the data of Table 1 which were intended to represent overall composition for the depth of the sample but which may have been weighted by material from one region of the sample, particularly the back of the layer. There is a decrease in the α-phase percentage content in going from the front surface to the back surface and a simultaneous increase in the β-phase content. When the sample is etched to remove excess silicon, it appears that all of the sample is sufficiently porous to allow the etchant to penetrate the layer. However, microscopic examination shows that the central region is still much more dense after etching than the bounding surface regions. After etching, the analysis shows that the α-phase content decreases from the front surface to the back surface while the β phase increases correspondingly. It also appears that the ratio of the β-phase content to the α-phase content is highest in the region where the silicon content is highest, suggesting that the β phase is the more stable phase in contact with molten silicon. A similar conclusion may also be inferred from other observations.

In one of our ribbon growth experiments the melt was raised to a higher temperature throughout the growth period (about 4 h) than in any previous runs. Subsequent examination of the die assembly (Si_3N_4 on vitreous carbon) revealed that the nitride layer (∿15 μm) was completely removed in the region of contact with molten silicon, and the vitreous carbon was strongly attacked. When residual silicon in the die was selectively etched away, it was found that β-Si_3N_4 needles and cubic SiC crystals (identified by x-ray diffraction) had formed at the ends of the V-shaped die where the temperature was lowest. The Si_3N_4 needles (see Fig. 3), were well defined, about 2 mm in length, and aligned in compact parallel clusters perpendicular to the triangular end pieces of the die. No evidence of α-Si_3N_4 was found among these clusters. Qualitatively, it appeared as if most of the dissolved nitride coating had reappeared in the form of β-Si_3N_4 needles. Analysis of the remaining layer outside the region of direct contact with the silicon melt showed the presence of both α and β phases. The only phases detected after etching away the silicon from the die were the three phases described. The temperature of the melt in this run is not known, but was probably close to 1500°C.

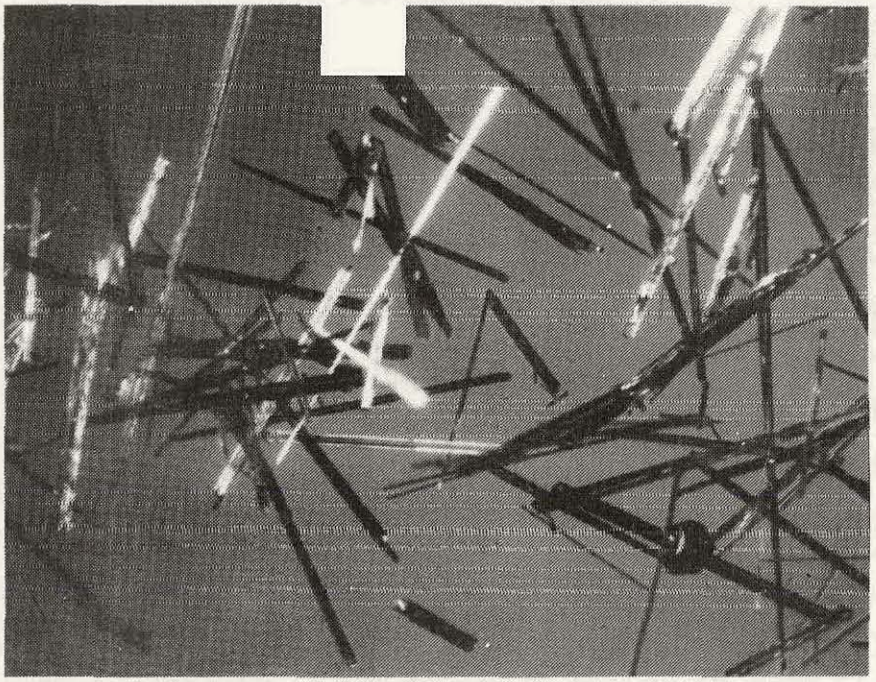

~70X

Figure 3. Micrograph of β-Si_3N_4 needles grown from the silicon melt on the cooler parts of the die assembly.

The values given in Tables 1 and 2 are very approximate and intended only as estimates of the composition changes occurring with high temperature treatment. There is also some uncertainty in the suitability of the sample used for purposes of analysis. We observed, during subsequent polishing of a portion of the same nitride slab, from which the above samples were taken, that the structure consisted of discrete layers which tended to peel off as a result of polishing. It became evident that a coherent layer cannot be obtained by successive depositions when the system is exposed to room ambient between depositions. The above results may be influenced by these observations, and other samples prepared in a single deposition step are now being evaluated. However, the trends are expected to be similar.

The analysis, to date, indicates that α-Si_3N_4 is an unstable form of Si_3N_4, whether alone or in contact with the melt, under the conditions likely to be encountered in silicon ribbon growth. The β phase appears, at this time, to be more stable under these conditions. Consequently, experiments are being directed toward the conversion of the α phase to the β phase prior to ribbon growth experiments. This requires information on the

rate of conversion as related to temperature and ambient. In preliminary experiments, a sample of Si_3N_4 (1 μm in thickness, NH_3:SiH_4 = 33:1 at 1000°C) on silicon was heated at 1400°C for 1 h in ultrapure He. The estimated composition of the film, as determined by x-ray diffraction, was about 90% α-Si_3N_4, and 10% β-Si_3N_4, based on the assumption that the film was completely crystallized. This sample was also used for transmission infrared measurements both before and after the heat treatment. The spectra, shown in Fig. 4, indicate typical amorphous character prior to heat treatment, Fig. 4(a), and crystalline character after annealing as revealed by the appearance of structure in the spectrum of Fig. 4(b). A point of interest here is that there is no evidence in these spectra for the existence of Si-H or N-H bonding in these films. The deposition conditions were originally chosen to avoid incomplete reaction of the starting materials. The result of this experiment indicates that, although crystallization is possible at 1400°C, the predominant phase is the α phase, and conversion to the β phase is very slow. To accelerate the conversion from the α to the β phase, portions of the same layer, used in the experiments corresponding to Tables 1 and 2 above, were heated to the 1600°C in N_2 for periods ranging from 1/4 to a total of 4-1/4 h. The purpose of the N_2 ambient was to suppress decomposition. As in Table 2, each sample was analyzed with respect to front surface, central region, and back surface. The results showed little difference in the content of these three regions for any sample, and little dependence on time in the range 1/4 to 4-1/4 h. In all cases the α:β ratio was approximately 2, and excess silicon was scarcely detectable in any sample (∿1%). Thus, nitrogen suppresses decomposition, but conversion from the α to β phase is still slow, apparently much slower than when in contact with the silicon melt for a given temperature. This is being studied further.

C. SILICON RIBBON GROWTH

Several silicon ribbon growth runs, using the V-shaped die configuration, were performed during this period. The dies were vitreous carbon coated with CVD-Si_3N_4. Considerable progress has been made in the thermal profile, and a number of ribbon segments with essentially constant width have been grown in consecutive runs. These were intentionally doped with boron during growth to about 1 Ω-cm for the fabrication of solar cells.

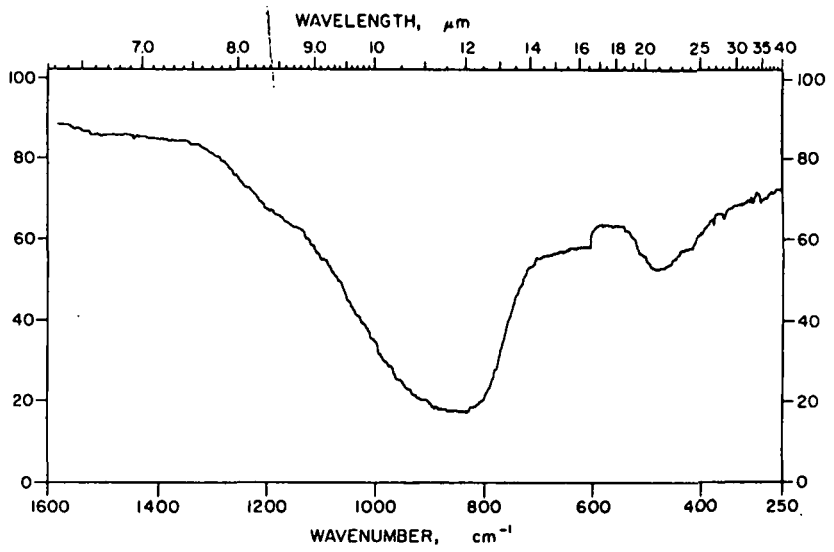

(a)

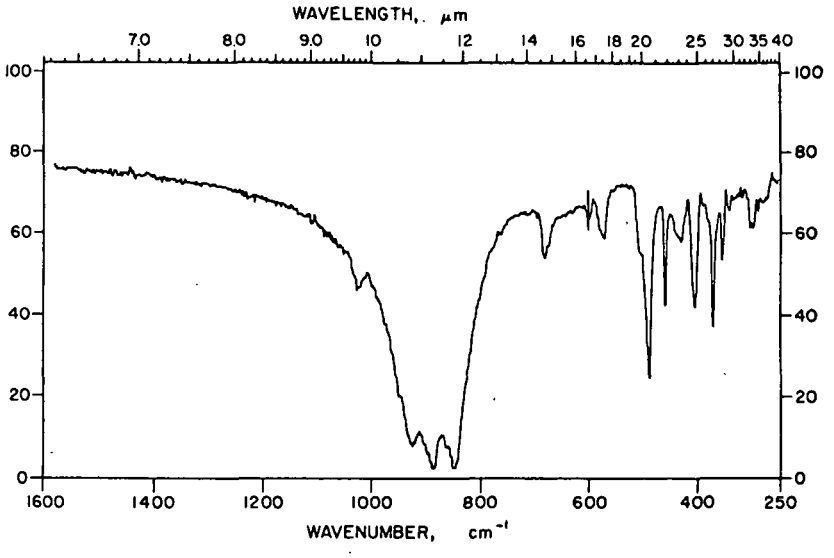

(b)

Figure 4. Transmission infrared spectra of CVD-Si_3N_4 corresponding to (a) amorphous as-prepared sample and (b) sample after crystallization at 1400°C in He for 1 h.

Two ribbons were evaluated for impurity content and defect structure prior to solar cell fabrication. Infrared transmission measurements were made on two such ribbons and on the seed material. The following results for oxygen and carbon were obtained.

TABLE 3. OXYGEN AND CARBON CONTENT OF RIBBON AND SEED MATERIALS

	Oxygen (ppma)	Carbon (ppma)
Seed	∿35	∿30-40
Ribbon	< 5	< 25

Measurements were made at several positions along the seed and ribbon in each case. The results here indicate that oxygen and carbon were not detected in the ribbon segments while these species were detected in the seed material. The values given for the ribbon are estimates of the detection level for the technique as employed here.

D. SOLAR CELL FABRICATION AND EVALUATION

Two silicon ribbon samples were fabricated into solar cells and evaluated by R. V. D'Aiello at RCA Laboratories. Two solar cells were made on each ribbon sample. For comparison, cells were also fabricated simultaneously on a control Czochralski silicon P-type wafer of 1.5 Ω-cm resistivity. The fabrication was conducted by first etching the surfaces of the ribbon to remove ∿1 mil from each side followed by a standard $POCl_3$ junction formation diffusion at 875°C for 25 min. The resulting sheet resistance of the junction layer for the ribbon and control samples were:

TABLE 4. SHEET RESISTANCE OF JUNCTION LAYER FOR RIBBON AND CONTROL SAMPLES AFTER JUNCTION FORMATION

Sample	Sheet Resistance (Ω/□)
R 2-1-78	60
R 2-1-78	57
R 2-10-78	48
R 2-10-78	49
Control	48

The samples were metallized with Ti/Ag on both sides and a standard comb pattern was defined on the junction surface. The cells were delineated with a mesa etch to linear dimensions of 1.15 cm x 2.0 cm. No AR coating was applied before the first measurement.

Measurements of the illuminated output characteristics were done with the ELH, AM-1, lamp simulator at 97 mW/cm^2. The resulting output curves and cell parameters are shown in Figs. 5-8. In addition, estimates of the lifetimes (diffusion length) were made from pulsed recovery measurements on small mesa diodes adjacent to the cells. These values are listed in Table 5.

TABLE 5. ESTIMATES OF LIFETIMES AND DIFFUSION LENGTHS FOR SAMPLES IN TABLE 4

Sample	Lifetime τ (μs)	Diffusion Length ($L = \sqrt{D\tau}$) (μm)
R 2-1-78	0.6	39
R 2-10-78	0.9	48
Control	3.6	95

Ribbon sample 2-10-78 was better in all respects than sample 2-1-78. The major difference was in the lifetime of diffusion length which results in the higher current and voltage for sample 2-10-78 and may be due to a higher contamination level in sample 2-1-78. Significant differences in surface texture between the two ribbon samples were noted before and after etching. Results obtained on sample 2-10-78, when a conventional single-layer AR coating (725 Å, ZrO_2) was applied, showed the following properties.

TABLE 6. RESULTS OF SOLAR CELL MEASUREMENTS ON SAMPLE R 2-10-78 WITH AND WITHOUT AR COATING

	No AR	AR
J_{sc} (mA/cm^2)	18.5	27.0
V_{oc} (mV)	550	562
η (%)	8.0	11.8
F.F.	0.767	0.769

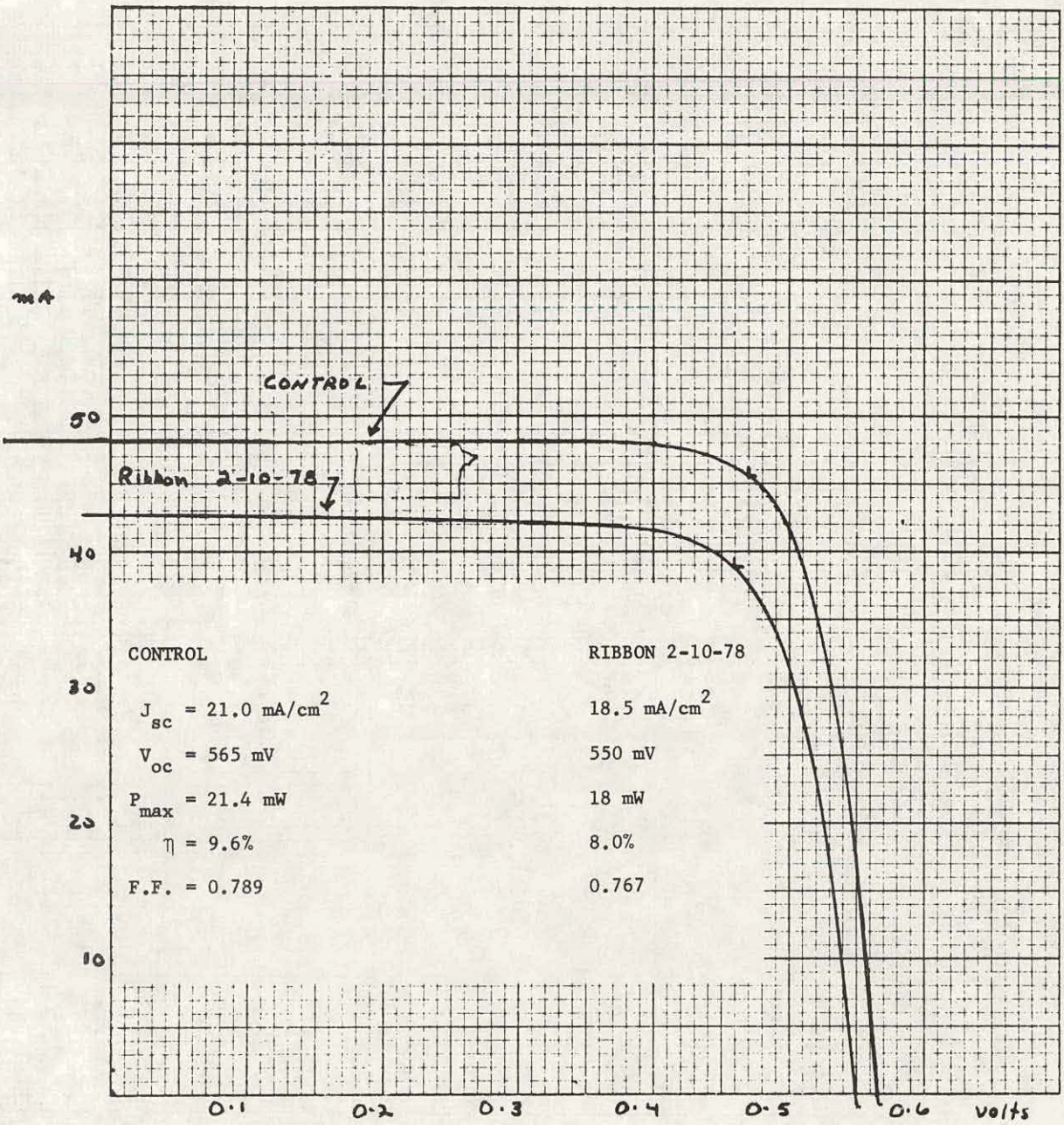

Figure 5. Solar cell characteristics for one of two cells on ribbon 2-10-78 and for control cell without AR coatings

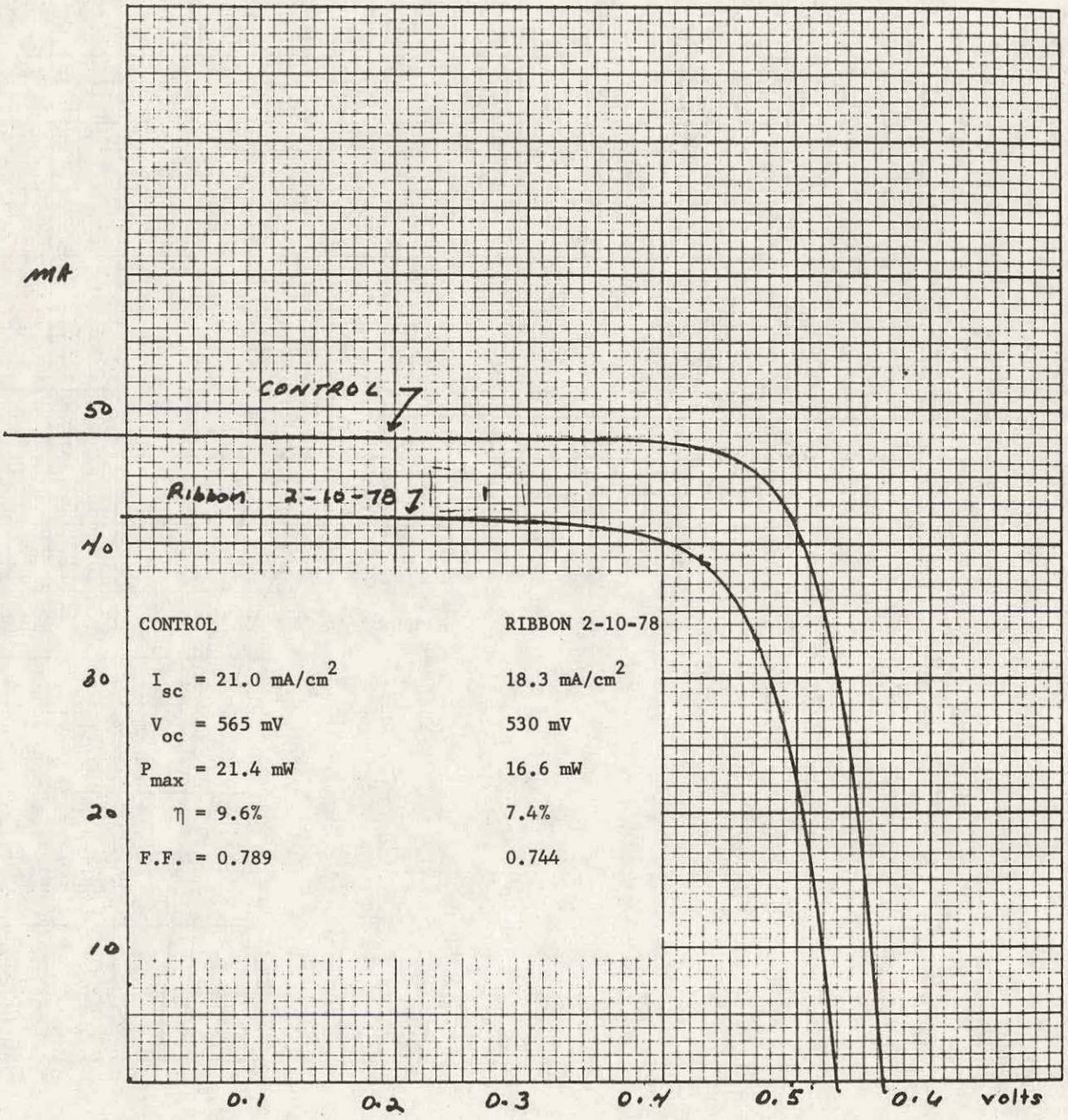

Figure 6. Solar cell characteristics for second cell on ribbon 2-10-78 and for control cell without AR coatings

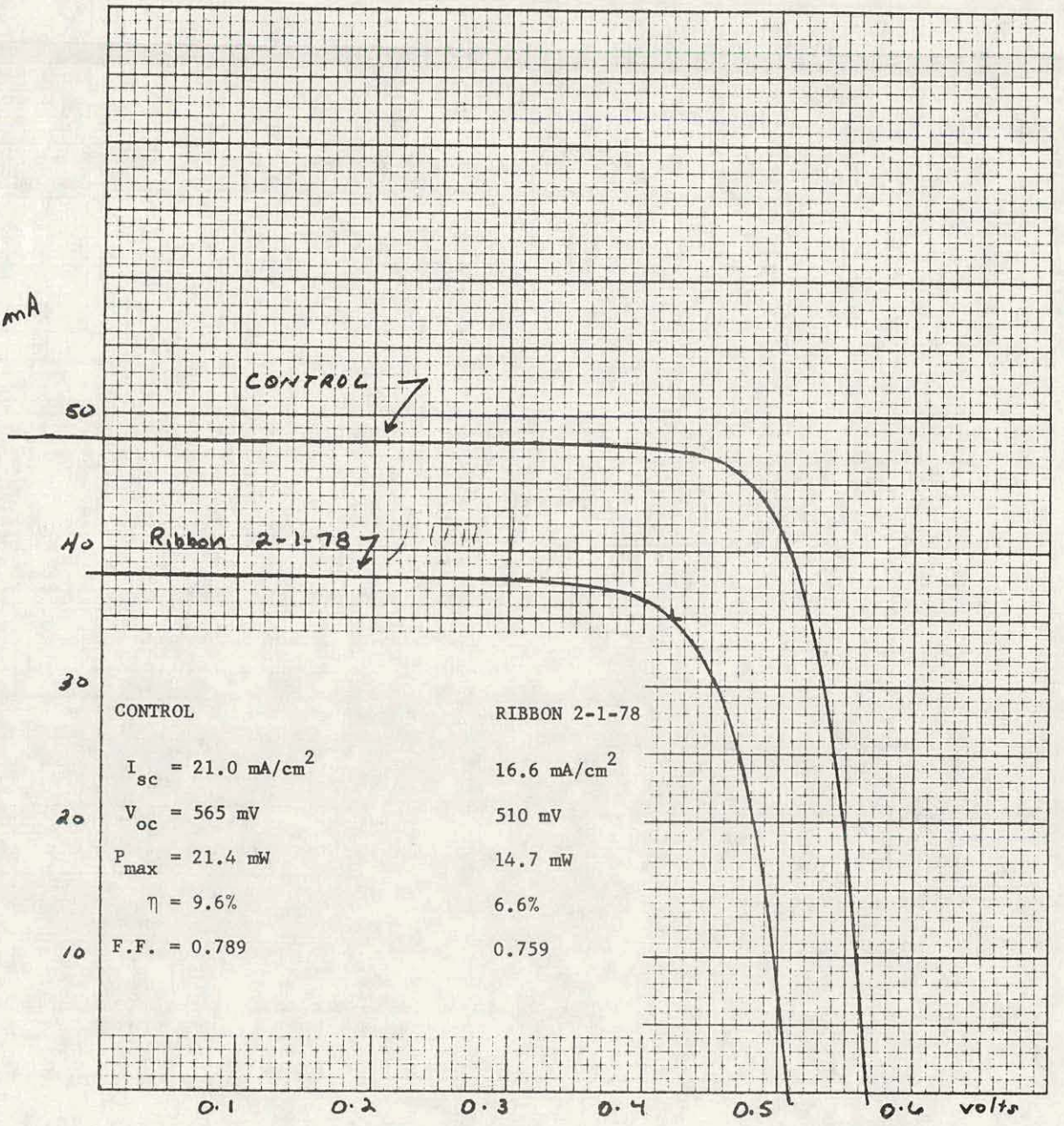

Figure 7. Solar cell characteristics for one of two cells on ribbon 2-1-78 and for control cell without AR coatings

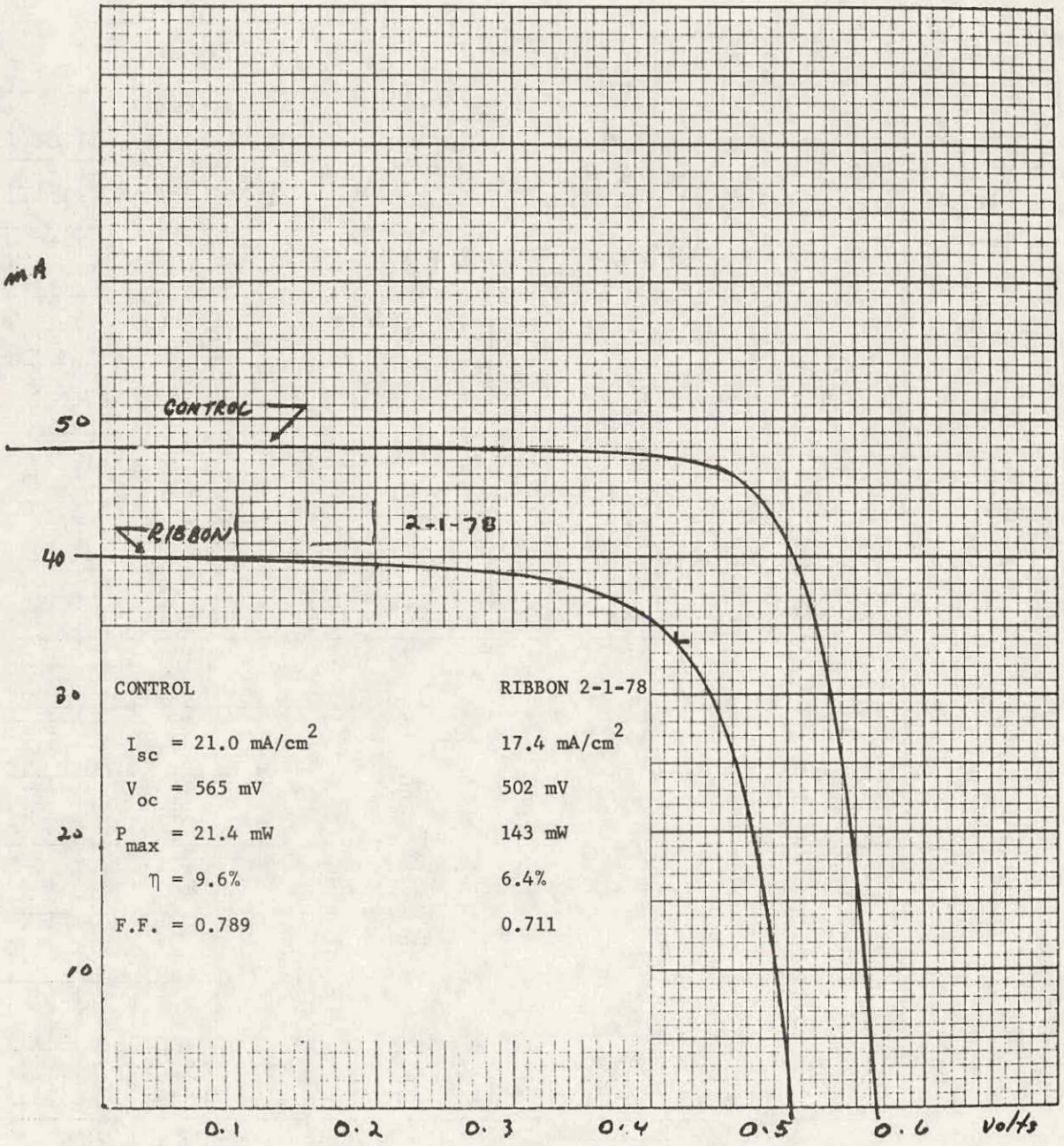

Figure 8. Solar cell characteristics for second cell on ribbon 2-1-78 and for control cell without AR coatings

SECTION IV

CONCLUSIONS AND FUTURE PLANS

Silicon sessile drop experiments on mullite and beryllia indicate that a CVD-Si_3N_4 layer on mullite can be useful in lowering the amount of dopant transferred from the substrate to the melt, while beryllia shows much less promise as a substrate material because of thermal expansion mismatch between substrate and CVD layer or solid silicon.

Results of x-ray analysis on the thermal stability of Si_3N_4, both in the presence and absence of molten silicon, show that the as-prepared amorphous layers are converted predominantly to the α phase with high-temperature treatment. The α phase is then slowly converted to the β phase accompanied by simultaneous decomposition. The latter process appears to occur more rapidly in contact with the silicon melt than in an inert gas. In both cases the β phase seems to be the more stable form of Si_3N_4. High-temperature ($\sim$1600°C) annealing in N_2 lowers the rate of decomposition, but conversion to the β phase is still slow.

Infrared analysis of silicon ribbon specimens grown from CVD-Si_3N_4 coated vitreous carbon dies showed that the oxygen and carbon levels were < 5 ppma for oxygen and < 25 ppma for carbon while the corresponding levels measured on the Czochralski seed material were $\sim$35 ppma for oxygen and 30-40 ppma for carbon. The best solar cell efficiency (without AR coatings) obtained on two such ribbons, was 8% as compared with 9.6% for a control sample. The efficiency was increased from 8 to 11.8% by the application of an AR coating.

We plan to continue the evaluation and analysis of CVD layers with special attention given to the formation of the β phase of Si_3N_4 prior to contact with molten silicon. The analysis of CVD-SiO_xN_y has commenced and will be evaluated in detail in the months ahead. Both materials will be used for the growth of silicon ribbon from the Mark II ribbon puller.

APPENDIX A

NEW TECHNOLOGY

There are no new technology items for this reporting period.

APPENDIX B

MILESTONES FOR DIE AND CONTAINER DEVELOPMENT

Key Tasks – Major Problems

1. Development and Evaluation of CVD-Si_3N_4-SiO_xN_y Systems
   - degradation and erosion rate of CVD-Si_3N_4 in contact with molten Si
   - optimization of CVD-Si_3N_4 as related to preparative conditions and post-deposition annealing
   - composition of as-deposited CVD-SiO_xN_y layers and identification of phases present after crystallization above the melting point of Si
   - degradation and erosion rate of CVD-SiO_xN_y in contact with molten Si
   - optimization with respect to preparative and annealing conditions
   - deposit above CVD layers on various die materials for the growth of silicon ribbon
   - fabricate self-supporting CVD dies and crucibles and test in contact with molten Si
2. Evaluation of Other CVD Coatings
   - identify other potentially useful coatings
   - prepare CVD coatings
   - test erosion in contact with molten Si
3. Reaction and Pressure-Sintered Materials for Use as CVD Substrates
   - Si_3N_4 with various densification aids
   - SiO_xN_y
   - Mullite
4. Characterization
   - materials characterization studies will be conducted according to that outlined in Articles 1 and 2 of Task Order No. RD-152
5. Inverted Ribbon Growth w/CVD Dies
   - Growth Rate
     - 50 cm/h
     - 100 cm/h
     - 150 cm/h
     - 200 cm/h
   - Thickness (±5 mil)
     - 40 mil
     - 30 mil
     - 20 mil
     - 15 mil
   - Ribbon Length (cm)
     - 10 cm
     - 15 cm
     - 20 cm
     - 30 cm
   - Operation of Mark I Puller
   - Operation of Mark II Puller

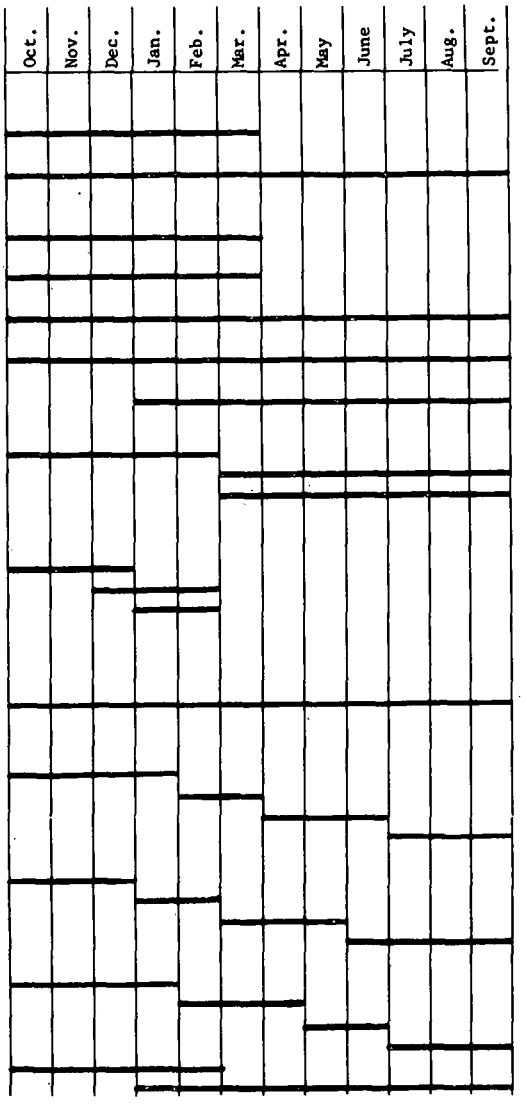

APPENDIX C

MANHOURS AND COSTS

Manhours and cost totals from October 1977 through February 1978 were 1,785 and $67,540, respectively.

☆U.S. GOVERNMENT PRINTING OFFICE: 1978-740-094/1446